

# Coulomb-gauge calculation of the combined effect of correlation and QED for heliumlike highly charged ions

J. Holmberg,<sup>1</sup> S. Salomonson,<sup>2</sup> and I. Lindgren<sup>2</sup><sup>1</sup>*Physikalisches Institut, Universität Heidelberg, Im Neuenheimer Feld 226, D-69120 Heidelberg, Germany*<sup>2</sup>*Department of Physics, University of Gothenburg, S-41296 Gothenburg, Sweden*

(Received 15 May 2015; published 9 July 2015)

We present numerical results for the energy shift due to the combination of Coulomb-correlation and quantum-electrodynamic effects in the ground state of heliumlike highly charged ions. The combined effect of two or more Coulomb interactions together with a single retarded photon, including radiative effects, is calculated for various atomic numbers in the range  $Z = 14$  to  $Z = 50$ . One step in our computational scheme involves the evaluation of the Coulomb-screened self-energy at the two-photon level, and we present a detailed comparison between the Coulomb and Feynman gauges with regard to the various contributions to this effect.

DOI: [10.1103/PhysRevA.92.012509](https://doi.org/10.1103/PhysRevA.92.012509)

PACS number(s): 31.30.J–

## I. INTRODUCTION

In highly charged ions relativistic and quantum-electrodynamic (QED) effects are pronounced due to the presence of the very strong nuclear potential. These systems are therefore well suited for accurate tests of fundamental theories in the strong-field regime, for example, by comparing observed and calculated bound-state transition energies.

Theoretical studies of the structure of heliumlike highly charged ions are undertaken with quite different methods depending on the size of the atomic number  $Z$ . For low  $Z$  it is essential to treat electron correlation accurately, either by the use of variational methods or some variant of many-body perturbation theory (MBPT). Corrections due to QED effects (retardation, self-interactions, and negative-energy states) cannot be included directly in these methods but have to be computed separately. Among the approaches that have been pursued to this end are various screening corrections to hydrogenic one-loop QED shifts due to local potentials [1–3] as well as the “unified method” of Drake [4].

In the high- $Z$  range, on the other hand, the relative importance of the electron-electron interaction is smaller while the QED effects become increasingly important, and in this region rigorous approaches based on bound-state QED are needed. To date, the most complete bound-state QED calculation was carried out in a comprehensive numerical study by Artemyev *et al.* [5], which is based on the “two-times Green’s function” method of Shabaev [6] and which includes all contributions up to the two-photon level for the  $n = 1$  and  $n = 2$  states in heliumlike ions in the range  $Z = 12$ –100. Two other methods for bound-state QED have been developed: the  $S$ -matrix formulation of Sucher [7], and the “covariant evolution-operator” method developed more recently by our group [8]. For practical reasons it is presently not possible to go beyond the two-photon level with any of these three approaches, and this means that a simultaneous treatment of QED effects and electron correlation<sup>1</sup> is currently beyond reach with these methods.

In order to study the combined effect of electron correlation and QED, which might be necessary to consider in an intermediate- $Z$  range, a scheme has been developed by our group where the QED effects can be included in an iterative perturbation expansion of the atomic wave function and energy. This is accomplished in the covariant evolution-operator framework by generalizing the standard relativistic many-body perturbation theory to include also energy-dependent perturbations, which is what the retarded nonlocal photons of QED constitute. We will in this paper present numerical results for the energy shift in the ground state of some heliumlike ions in the range  $Z = 14$ –50 due to the combined effect of correlation and single-photon QED effects (self-energy, vacuum polarization, and retarded single-photon exchange) obtained with this method.

## II. THEORY

### A. Energy-dependent many-body perturbation theory

The photon-mediated processes of bound-state QED correspond to  $N$ -electron operators (for example,  $N = 1$  in the case of the electron self-energy and  $N = 2$  for single photon exchange) which can be considered as perturbations to bound electron states. Due to the retarded nature of the photon they will in general be energy-dependent perturbations and in order to include them in a perturbation expansion of energy shifts and corrections to wave functions we will rely on the energy-dependent many-body perturbation theory developed in [8–12] based on the covariant evolution-operator formalism. We will here only summarize the main results of this theory as it applies to the atomic problem.

Let  $|\Psi\rangle$  denote an exact, stationary state with energy  $E$ , which includes the interaction among  $N$  electrons bound to an (infinitely heavy) atomic nucleus as well as their self-interactions. A so-called *model state*  $|\Psi^{(0)}\rangle$  with energy  $E^{(0)}$  serves as a zeroth-order approximation to  $|\Psi\rangle$ . The model state lies in a *model space* and is constructed from a linear combination of eigenstates  $|\phi_\alpha^{(0)}\rangle$  to a *model Hamiltonian*  $H_0$ ,

$$H_0|\phi_\alpha^{(0)}\rangle = E_\alpha^{(0)}|\phi_\alpha^{(0)}\rangle, \quad (1)$$

<sup>1</sup>In this work we will refer to effects containing at least two electron-electron interactions as correlational effects.

which typically includes the interaction of the individual electrons with the nuclear potential and perhaps some mean-field interaction term between the electrons. We will in the following for simplicity assume that the model space is one-dimensional, although the formalism can be extended to include multidimensional model spaces containing more than one energy [9].

The exact state can be generated from its model state via the energy-dependent Green's operator  $\mathcal{G}(\mathcal{E}, t)$

$$|\Psi\rangle = \mathcal{G}(E^{(0)}, 0)|\Psi^{(0)}\rangle, \quad (2)$$

evaluated at time  $t = 0$ . The Green's operator, which contains the interaction between the electrons and their self-interactions, is formally defined in terms of a relativistic time-evolution operator and can be constructed perturbatively using quantum field theory [9,12]. For our present purposes we will use the fact that a large part of  $\mathcal{G}$  can be written as a time-ordered perturbation expansion in terms of energy-dependent, photon-mediated perturbations  $V(\mathcal{E})$ :

$$\mathcal{G}(\mathcal{E}, t) = \mathcal{G}_0(\mathcal{E}, t) + \sum_{n=1}^{\infty} \frac{\delta^n \mathcal{G}_0(\mathcal{E}, t)}{\delta \mathcal{E}^n} W^n, \quad (3)$$

where

$$\mathcal{G}_0(\mathcal{E}, t) = e^{-it(\mathcal{E}-H_0)} \left[ 1 + \sum_{n=1}^{\infty} \{\Gamma_Q(\mathcal{E})V(\mathcal{E})\}^n \right] \quad (4)$$

is that part of  $\mathcal{G}$  whose perturbation-expansion contains no model-space states.  $\Gamma_Q$  is the *reduced resolvent*

$$\Gamma_Q(\mathcal{E}) = \frac{Q}{\mathcal{E} - H_0}, \quad (5)$$

which operates only in the *complementary space* with projection operator  $Q$ , orthogonal to the model space with projection operator  $P$ .

$W$  is the *effective interaction*

$$W(\mathcal{E}) = P \left( i \frac{\partial}{\partial t} \mathcal{G}(\mathcal{E}, t) \right)_{t=0} P, \quad (6)$$

which gives the energy shift

$$W(E^{(0)})|\Psi^{(0)}\rangle = (E - E^{(0)})|\Psi^{(0)}\rangle = \Delta E|\Psi^{(0)}\rangle. \quad (7)$$

The difference ratio  $\delta^n \mathcal{G} / \delta \mathcal{E}^n$  appearing in Eq. (3) is discussed in detail in Appendix B of [10], and for  $n = 1$  it turns into an ordinary derivative

$$\frac{\delta \mathcal{G}}{\delta \mathcal{E}} \rightarrow \frac{\partial \mathcal{G}}{\partial \mathcal{E}} \quad (8)$$

in the case of a model space containing only a single energy.

Equation (3) generates a so-called ladder-expansion of  $\mathcal{G}$  in which the perturbations  $V(\mathcal{E})$  do not overlap in time. All contributions from intermediate model states are given by the second term in Eq. (3) and we denote these as *model-space contributions* (MSC). They are a generalization of the so-called folded terms in standard many-body perturbation theory (see, e.g., [13]) to which they reduce when the perturbation  $V$  is energy independent.

In the following we will use the designation *wave operator* for the Green's operator at time  $t = 0$  and denote it by

$$\mathcal{G}(\mathcal{E}, t = 0) = \Omega. \quad (9)$$

This is in accordance with the notation used in standard (energy-independent) many-body perturbation theory. Note that in the case of a one-dimensional model space considered here, the energy dependence of  $\mathcal{G}$  (and therefore also  $\Omega$ ) is given by the energy  $E^{(0)}$  of the model state it acts on.

A convenient form of the effective interaction (6) for practical calculations is

$$W^{(n)} = P \tilde{\Omega}^{(n)} P, \quad (10)$$

where  $\tilde{\Omega}^{(n)}$  is the  $n$ th-order wave operator without its final resolvent:

$$\Omega^{(n)} = \Gamma_Q \tilde{\Omega}^{(n)}. \quad (11)$$

### B. Application to the ground state of heliumlike ions

A suitable model Hamiltonian for a heliumlike system is the sum

$$H_0 = \sum_{i=1}^2 [\alpha \cdot \hat{\mathbf{p}}_i + \beta m + V_{\text{nuc}}(r_i)] \quad (12)$$

of two single-electron Dirac Hamiltonians including the attractive nuclear potential  $V_{\text{nuc}}$ . The interaction between the pair of electrons as well as their self-interactions are described by  $V(\mathcal{E})$  which we will here take to be

$$V(\mathcal{E}) = V_{\text{PE}}(\mathcal{E}) + V_{\text{SE}}(\mathcal{E}) + V_{\text{VP}}. \quad (13)$$

The first term on the right-hand side of Eq. (13) is the operator for single-photon exchange between the electrons which in Coulomb gauge has the form

$$V_{\text{PE}}^{\text{Coul}}(\mathcal{E}) = V_C + V_T(\mathcal{E}). \quad (14)$$

Here,  $V_C$  is the instantaneous Coulomb interaction (which carries no energy dependence) and  $V_T(\mathcal{E})$  is the transverse part of the interaction which includes the retardation effect. We will in the following use the Coulomb gauge for all photon exchanges between the electrons.

The second term in Eq. (13) is given by the mass-renormalized one-loop self-energy operator  $\Sigma$  and the third term is given by the (energy-independent) charge-renormalized single-electron vacuum-polarization potential. This choice of  $V(\mathcal{E})$  corresponds to considering only one-photon perturbations (see Fig. 1).

The Coulomb interaction  $V_C$  can be treated numerically to essentially all orders using standard many-body perturbation theory and it represents most of the interelectron interaction. By separating out  $V_C$  from the single-photon exchange operator we write  $V(\mathcal{E})$  as

$$V(\mathcal{E}) = V_C + V_{\text{QED}}(\mathcal{E}), \quad (15)$$

where

$$V_{\text{QED}}(\mathcal{E}) = V_T(\mathcal{E}) + V_{\text{SE}}(\mathcal{E}) + V_{\text{VP}} \quad (16)$$

contains the energy-dependent QED effects which cannot be handled with the standard (energy-independent) MBPT.

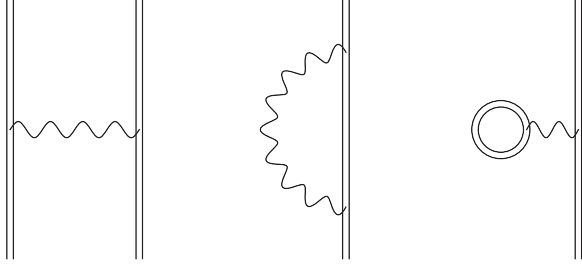


FIG. 1. The one-photon perturbations in bound-state QED, from left to right: single-photon exchange, self-energy, and vacuum polarization. The double lines denote electrons propagating in the nuclear electrostatic potential and the wavy lines denote photons.

In order to compute the combined effect of QED and correlation we wish to treat  $V_C$  to high order while retaining the QED effects (retardation and radiative corrections) to lowest order (a single retarded photon). To achieve this it is convenient to formulate an iterative equation for the wave operator  $\Omega$  where the Coulomb interaction is included recursively but the QED effects appear in a nonrecursive way. Such an equation is derived in [9] and [14] and it can be written as

$$\begin{aligned} \Omega_1^{\text{1ph}} = & \Gamma_Q V_C \Omega_1^{\text{1ph}} - \Gamma_Q \Omega_1^{\text{1ph}} W_1 - \Gamma_Q \Omega_1 W_1^{\text{1ph}} \\ & + \Gamma_Q V_{\text{QED}} \Omega_1 + \Gamma_Q \sum_{n=1}^{\infty} \frac{\delta^n V_{\text{QED}}}{\delta \mathcal{E}^n} \Omega_1 (W_1)^n. \end{aligned} \quad (17)$$

Here the subscript I stands for “instantaneous” and denotes a complete ladder sequence of instantaneous interactions.  $\Omega_1$  is a self-consistently generated, energy-independent wave operator containing *only* instantaneous Coulomb interactions,

$$\Omega_1 = \Gamma_Q V_C \Omega_1 - \Gamma_Q \Omega_1 W_1, \quad (18)$$

and  $\Omega_1^{\text{1ph}}$  is that part of the full, energy-dependent wave operator which contains precisely one retarded photon together with arbitrarily many Coulomb interactions.<sup>2</sup>

$\Omega_1^{\text{1ph}}$  is included recursively in the first three terms on the right-hand side of Eq. (17), and by iteratively updating the right-hand side these terms will generate a series of Coulomb interactions (including folded terms) *after* the retarded photon. The last two terms of Eq. (17), on the other hand, introduce the QED effects to the instantaneous wave operator precisely once, and this means that they will only appear linearly in  $\Omega_1^{\text{1ph}}$ , in between the Coulomb interactions contained in  $\Omega_1$  and those that are generated afterward (see Fig. 4).

A numerical implementation of Eq. (17) can be accomplished by using the spectral representation of  $\Gamma_Q$ :

$$\Gamma_Q(\mathcal{E}) = \sum_{rs \neq ab} \frac{|rs\rangle \langle rs|}{\mathcal{E} - \varepsilon_r - \varepsilon_s}, \quad (19)$$

where  $|rs\rangle$  is an eigenstate of  $H_0$  with energy  $\varepsilon_r + \varepsilon_s$ , and acting with the resulting operator to the right on the model

<sup>2</sup>The full wave operator is in this scheme written as an expansion in terms of the number of retarded photons together with arbitrarily many Coulomb interactions:  $\Omega = 1 + \Omega_1 + \Omega_1^{\text{1ph}} + \Omega_1^{\text{2ph}} + \dots$ .

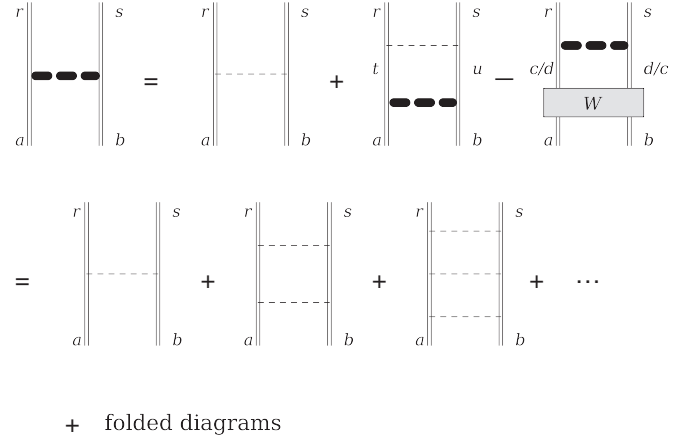


FIG. 2. The pair equation in diagrammatic form. The thin dashed lines represent the Coulomb interaction and the heavy dashed lines represent the accumulated effect of correlation. The last term of the top row (the “folded” term) is given in the general form which allows for intermediate model states  $|cd\rangle$  which may be different from  $|ab\rangle$  (an extended model space). Iterating this equation until convergence gives the ordinary pair function  $|\rho_{ab,1}\rangle$  which contains an infinite ladder of Coulomb interactions including folded terms.

state  $|1s1s\rangle \equiv |ab\rangle$ . This gives, for a particular outgoing  $\langle rs|$ , the equation

$$\begin{aligned} & (\varepsilon_a + \varepsilon_b - \varepsilon_r - \varepsilon_s) \langle rs | \rho_{ab,1}^{\text{1ph}} \rangle \\ & = \langle rs | V_C | \rho_{ab,1}^{\text{1ph}} \rangle - \langle rs | \rho_{ab,1}^{\text{1ph}} \rangle W_1 - \langle rs | \rho_{ab,1} \rangle W_1^{\text{1ph}} \\ & + \langle rs | V_{\text{QED}} | \Psi_{ab,1} \rangle + \sum_{n=1}^{\infty} \langle rs | \frac{\delta^n V_{\text{QED}}}{\delta \mathcal{E}^n} | \Psi_{ab,1} \rangle (W_1)^n. \end{aligned} \quad (20)$$

Here,

$$|\Psi_{ab,1}\rangle = \Omega_1 |ab\rangle = |ab\rangle + |\rho_{ab,1}\rangle \quad (21)$$

is the *extended pair function*, which includes the model state as well as the correction  $|\rho_{ab,1}\rangle$  due to Coulomb correlation between the electrons. The correction  $|\rho_{ab,1}\rangle$  (the “ordinary” pair function) is the solution to the pair equation [15]

$$|\rho_{ab,1}\rangle = \Gamma_Q V_C |ab\rangle + \Gamma_Q V_C |\rho_{ab,1}\rangle - \Gamma_Q |\rho_{ab,1}\rangle W_1, \quad (22)$$

which is the result of acting with Eq. (18) on  $|ab\rangle$  using Eq. (21). The pair equation is shown in diagrammatic form in Fig. 2. The extended pair function is shown in Fig. 3.

The function

$$|\rho_{ab,1}^{\text{1ph}}\rangle = \Omega_1^{\text{1ph}} |ab\rangle \quad (23)$$

is a Coulomb-correlated pair function containing precisely one retarded photon (see Fig. 4). It is the correction to  $|ab\rangle$  due to the combined effects considered in Eq. (20).

The energy-shift associated with  $\Omega_{ab,1}^{\text{1ph}}$  is computed with the effective interaction (10), and is given by the right-hand side of (20) with  $\langle rs|$  replaced by  $\langle ab|$ . In order to isolate the effects which lie beyond the two-photon level we compute the difference

$$\Delta E_{\text{QED-corr.}} = \Delta E_1^{\text{1ph}} - \Delta E^{\text{1ph}} - \Delta E_{\text{1C after}}^{\text{1ph}} - \Delta E_{\text{1C before}}^{\text{1ph}} \quad (24)$$

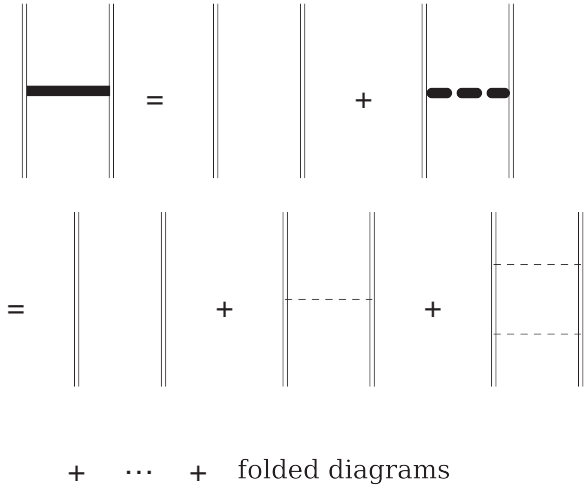


FIG. 3. The extended pair function  $|\Psi_{ab,1}\rangle = |ab\rangle + |\rho_{ab,1}\rangle$  is equal to the exact two-electron state in the (no-virtual-pair) Coulomb approximation.

where  $\Delta E_I^{1\text{ph}}$  is the energy shift due to the fully correlated one-photon wave operator  $\Omega_{ab,1}^{1\text{ph}}$ ,  $\Delta E^{1\text{ph}}$  is the energy shift due to the single-photon perturbation alone, and  $\Delta E_{1\text{C before}}^{1\text{ph}}$  and  $\Delta E_{1\text{C after}}^{1\text{ph}}$  are the energy shifts for a single photon together with one Coulomb interaction (before and after, respectively). The subtraction is illustrated for the self-energy case in Fig. 5.

The energy shifts for the second-order terms (a single-photon plus one Coulomb interaction) can be compared with

results at the two-photon level from the literature and thus serve as a test of our method. In particular, our calculation involves a numerical evaluation of the Coulomb-screened self-energy shift in Coulomb gauge, and a detailed comparison of the different contributions to this shift between Coulomb and Feynman gauge can be carried out.

### III. METHOD

We obtain a numerical basis set by solving the radial Dirac equation including the electrostatic nuclear potential on a discretized grid [16]. This allows a straightforward inclusion of the nuclear-size effect directly into the radial wave functions by modifying the  $1/r$  dependence of the potential inside the nuclear radius. In this work we model the nucleus as a homogeneous, spherical charge distribution of radius  $R_{\text{nuc}}$ ; see Table I for the nuclear radii used in our calculations.

The numerical realization of Eq. (20) involves the computation of matrix elements of the various interactions (and their derivatives) with respect to the numerical basis functions. The spin-angular integrations can for the most part be performed analytically using partial-wave expansions and graphical angular-momentum techniques (see [13] for details regarding angular-momentum graphs), while the radial integrals are performed numerically. The calculations are performed for a series of radial grids with increasing resolution and the results are extrapolated to continuous space. The partial-wave expansions are necessarily truncated and an extrapolation to infinite summation limits is performed.

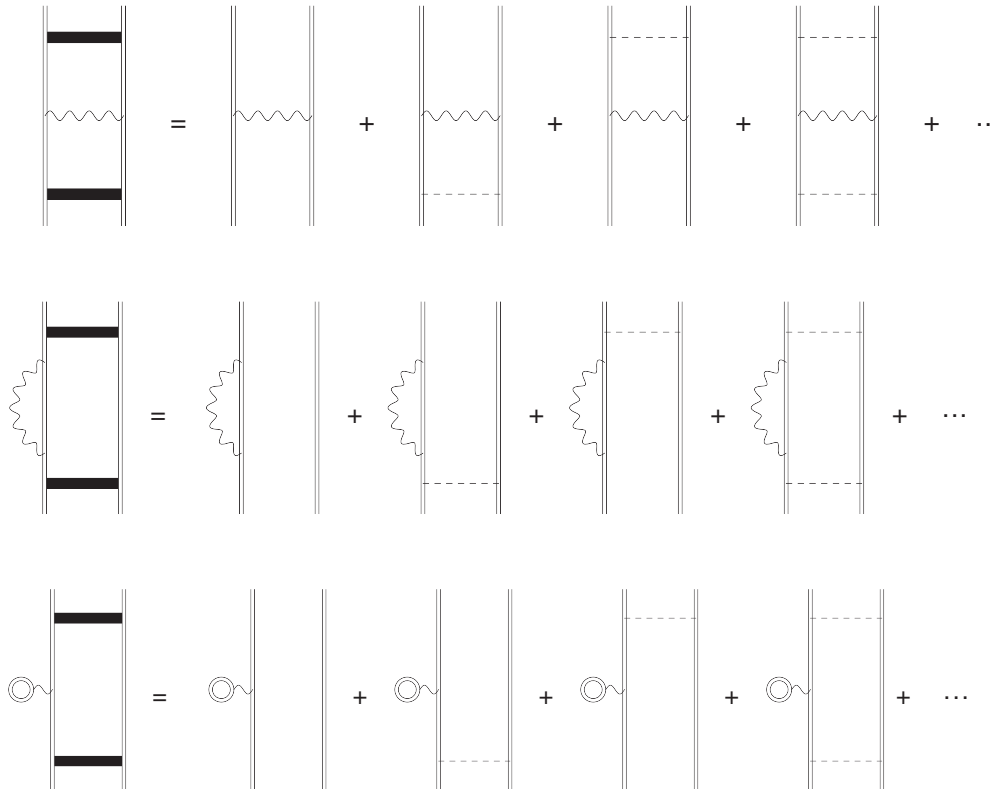


FIG. 4. Three different pair functions containing a single retarded photon (photon exchange, self-energy, or vacuum polarization) together with arbitrarily many Coulomb interactions including model-space contributions.

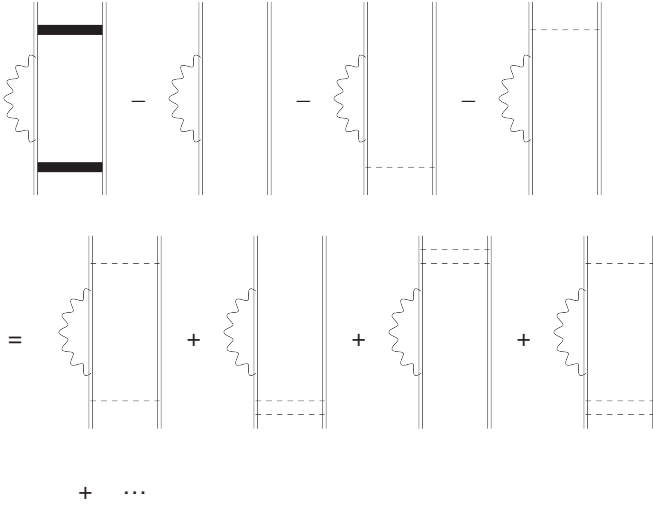


FIG. 5. Effects beyond the two-photon level (correlational effects) are calculated as the difference between the energy shift due to the fully correlated one-photon wave operator and the three lowest-order approximations.

The matrix elements of the Coulomb interaction are well known and can be put in the form

$$\langle rs|V_C|tu\rangle = \sum_{k=0}^{\infty} (-1)^k \langle j_r||\mathbf{C}^k||j_t\rangle \langle j_s||\mathbf{C}^k||j_u\rangle R_k A_1, \quad (25)$$

where  $j_r$  is the total angular-momentum quantum number of the state  $|r\rangle$ ,  $R_k$  is a radial Slater integral,  $\mathbf{C}^k$  is a spherical tensor of rank  $k$ , and  $A_1$  is an angular-momentum factor. The radial integrals are performed using Lagrange interpolation of the basis functions between grid points, and  $A_1$  is computed using angular-momentum graphs.

The matrix elements of  $V_T(\mathcal{E})$  for positive-energy states are [9,17]

$$\begin{aligned} \langle rs|V_T(\mathcal{E})|tu\rangle &= \langle rs|\int_0^{\infty} dk f_T(\mathbf{x}_1, \mathbf{x}_2, k) \left[ \frac{1}{\mathcal{E} - \varepsilon_r - \varepsilon_u - (k - i\delta)} \right. \\ &\quad \left. + \frac{1}{\mathcal{E} - \varepsilon_s - \varepsilon_t - (k - i\delta)} \right] |tu\rangle, \end{aligned} \quad (26)$$

where  $k$  is the linear momentum of the photon, and the  $f_T$  function for the transverse part of the Coulomb-gauge

TABLE I. The nuclear radii used in this work. We model the nucleus as a homogeneous spherical charge distribution.

| Z  | Nuclear radius (fm) |
|----|---------------------|
| 14 | 3.123               |
| 18 | 3.423               |
| 24 | 3.643               |
| 30 | 3.928               |
| 50 | 4.654               |

interaction is

$$\begin{aligned} f_T(\mathbf{x}_1, \mathbf{x}_2, k) &= -\frac{e^2}{4\pi^2\epsilon_0} \left[ -\boldsymbol{\alpha}_1 \cdot \boldsymbol{\alpha}_2 \frac{\sin(kr_{12})}{r_{12}} \right. \\ &\quad \left. + (\boldsymbol{\alpha}_1 \cdot \nabla_1)(\boldsymbol{\alpha}_2 \cdot \nabla_2) \frac{\sin(kr_{12})}{k^2 r_{12}} \right]. \end{aligned} \quad (27)$$

This expression can be generalized to allow also for negative-energy states [9], the square bracket in Eq. (26) should then be replaced with

$$\begin{aligned} &\pm \frac{t_{\pm} r_{\mp}}{\varepsilon_t - \varepsilon_r \pm (k - i\delta)} \pm \frac{u_{\pm} s_{\mp}}{\varepsilon_u - \varepsilon_s \pm (k - i\delta)} \\ &\pm \frac{t_{\pm} s_{\pm}}{\mathcal{E} - \varepsilon_t - \varepsilon_s \mp (k - i\delta)} \pm \frac{u_{\pm} r_{\pm}}{\mathcal{E} - \varepsilon_r - \varepsilon_u \mp (k - i\delta)}. \end{aligned} \quad (28)$$

Here  $t_+$  ( $t_-$ ) is a projection operator for positive-energy (negative-energy)  $t$  states and similarly for the other states. The upper or lower sign should be used consistently in each term.

The expression (26) contains a part which is energy independent and which is known as the *instantaneous Breit interaction*:

$$V_{IB} = -\frac{e^2}{4\pi\epsilon_0} \left[ \frac{\boldsymbol{\alpha}_1 \cdot \boldsymbol{\alpha}_2}{r_{12}} + \frac{1}{2}(\boldsymbol{\alpha}_1 \cdot \nabla_1)(\boldsymbol{\alpha}_2 \cdot \nabla_2)r_{12} \right]. \quad (29)$$

This part can be included in a perturbation expansion based on standard MBPT and normally one considers the correction due to retardation, which is the difference between the full interaction (26) and the instantaneous part (29), as a genuine QED effect.

In analogy with the Coulomb interaction, the matrix elements (26) are expanded into a sum of partial waves

$$\frac{\sin(kr_{12})}{kr_{12}} = \sum_{l=0}^{\infty} (2l+1) j_l(kr_1) j_l(kr_2) \mathbf{C}_1^l \cdot \mathbf{C}_2^l, \quad (30)$$

where  $l$  is the orbital angular momentum of the photon and  $j_l$  are spherical Bessel functions, and also here the spin-angular integrals can be treated using graphical methods. For each  $k$  the remaining radial integrals are performed using Lagrange interpolation together with recursion relations for integrals  $I_l^m$  over products  $r^m j_l(kr)$  of spherical Bessel functions and powers of  $r$ . The final integration over  $k$  is performed using Gauss-Legendre quadrature with a finite cutoff at large momenta.

The two-electron matrix elements of the (mass-renormalized) single-electron self-energy operator  $\Sigma$  are

$$\langle rs|V_{SE}(\mathcal{E})|tu\rangle = \delta_{u,s} \langle r|\Sigma(\mathcal{E} - \varepsilon_u)|t\rangle. \quad (31)$$

The matrix elements are computed using the standard expansion in terms of scattering order with the nuclear potential into zero-, one-, and many-potential terms [18,19] (see Fig. 6), and their Coulomb-gauge expressions are given in [20] and [21]. The zero- and one-potential terms, which are computed in momentum space, can in principle be obtained using the Fourier transformations of the in- and outgoing single-electron states  $|t\rangle$  and  $|r\rangle$ . However, the highly excited discretized radial solutions acquire considerable contributions from a wide range of large momenta, and due to the oscillatory behavior and slow decay of the integrands it is challenging to perform

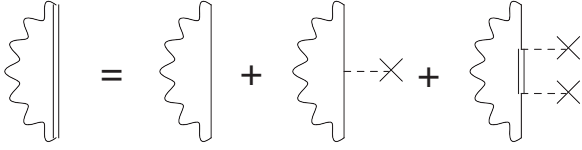


FIG. 6. Expansion of the bound self-energy operator in terms of scattering order with the nuclear potential. The thin straight lines correspond to freely propagating electrons, and the dashed lines with a cross represent the Coulomb potential from the nucleus.

the numerical integration without introducing large numerical errors. Much can be gained by instead working directly with the single-coordinate radial representations of the incoming pair function  $\langle r_1 | \rho_{ab,1} \rangle$  and outgoing resolvent

$$\Gamma_Q(\mathcal{E} - \varepsilon_u, r_1, r'_1) = \sum_n \frac{\langle r'_1 | n \rangle \langle n | r_1 \rangle}{\mathcal{E} - \varepsilon_u - \varepsilon_n}, \quad (32)$$

which are both relatively smooth and localized and whose Fourier transforms decay quite rapidly. The numerical Fourier transformations are computed similarly to the radial integrals described above for the single-photon exchange, and the integration over the momentum variables is performed using Gauss-Legendre quadrature. The one-potential term contains additional integrals over Feynman parameters as well as over an angle between the incoming and outgoing momenta. Some of the Feynman-parameter integrals can be performed analytically [21], the remaining ones and the angular integral are performed numerically.

The radial vacuum-polarization potential  $V_{VP}(r)$  in Eq. (13) contains two parts. The Uehling potential, which is the  $n = 1$  term in a  $Z\alpha$  expansion of the electron propagator in the loop (the even terms vanish due to Furry's theorem), can be written as [22]

$$\begin{aligned} U_{\text{Ueh}}(r) = & -\frac{e^2}{4\pi\epsilon_0} \frac{\alpha}{\pi} \int_0^\infty dr' 4\pi r'^2 \rho_{\text{nuc}}(r') \\ & \times \int_1^\infty dt \sqrt{t^2 - 1} \left( \frac{2}{3t^2} + \frac{1}{3t^4} \right) \\ & \times \frac{\sinh(4\pi t r_{<}/\lambda_C)}{4\pi t r_{<}/\lambda_C} \frac{e^{-4\pi t r_{>}/\lambda_C}}{r_{>}}, \end{aligned} \quad (33)$$

where  $\rho_{\text{nuc}}$  is the nuclear charge distribution,  $r_{<}$  ( $r_{>}$ ) is the lesser (greater) of the radial coordinates, and  $\lambda_C = h/(mc)$  is the Compton wavelength of the electron. The remaining Wichmann-Kroll part, which contains all higher-order terms, can be computed approximately using the formulas given in [23].

The model-space contributions (MSCs) involve energy derivatives of the perturbations. We will in this work only consider the  $n = 1$  term in Eq. (20) and neglect the higher-order derivatives. The energy derivative of the transverse-photon interaction can be calculated in the same way as Eq. (26) with the only difference being the power of the denominators and the overall sign:

$$\frac{1}{\mathcal{E} - \varepsilon_t - \varepsilon_u - k} \rightarrow \frac{-1}{(\mathcal{E} - \varepsilon_t - \varepsilon_u - k)^2}. \quad (34)$$

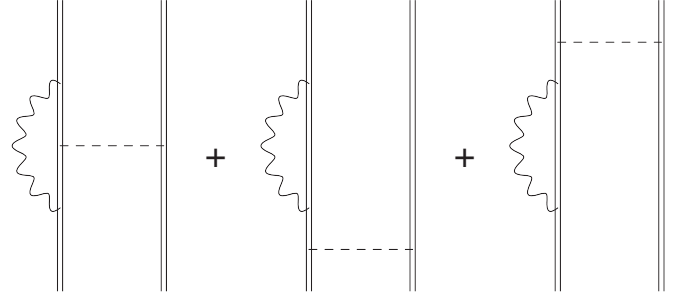


FIG. 7. The complete, gauge-invariant Coulomb-screened self-energy at the two-photon level. The leftmost diagram is the vertex correction. The two remaining terms contain the wave-function correction (only intermediate  $Q$ -space states) and the model-space contribution (MSC). The vertex correction has to be considered together with the MSC due to the cancellation of their respective divergent terms.

The energy-derivative of the self-energy operator is more troublesome since it contains a UV divergence. At the two-photon level this divergence cancels against a corresponding term in the *vertex correction* (the leftmost term in Fig. 7) which is a nonseparable two-photon effect. We have not been able to explicitly demonstrate this cancellation in higher orders, but assuming that the divergences do cancel separately in each order we may simply use the renormalized, finite expressions for the corresponding operators in our perturbation expansion.

Unfortunately, the full evaluation of the two-electron matrix elements of the vertex correction has to be performed individually for each combination of in- and outgoing states since their energies all appear in the integral, and this becomes prohibitively time consuming in the general case. However, our analysis of the Coulomb-screened self-energy at the two-photon level (see Table II) suggests that in the Coulomb gauge we can obtain a reasonable approximation to the full evaluation of the self-energy MSC plus vertex correction by simply neglecting the “higher-order terms.” These terms are the remainders after subtracting away the zero-potential terms which correspond to freely propagating electrons inside the photon loops in Fig. 7. The zero-potential terms can be computed without difficulty even in the fully correlated case, and this enables us to obtain approximative results for the self-energy MSC and vertex-correction contributions in the Coulomb gauge, again assuming that the cancellation of divergences proceeds in a straightforward way in the perturbation expansion. The Feynman gauge, on the other hand, would require evaluation also of the higher-order terms since there are very large cancellations among the terms in this gauge.

Our calculation of the vertex correction and self-energy MSC is carried out in a similar way as that described in [24] and proceeds as follows. The cancellation of UV divergences between the vertex correction and self-energy MSC is handled with dimensional regularization following an expansion of the bound electron propagators in terms of scattering order with the nuclear potential. The UV-divergent quantities are located in the zero-potential terms and the finite remainders after cancellation are computed in momentum space as expectation values of the corresponding renormalized free-electron operators. The remaining higher-order contribution is com-

TABLE II. Contributions to the Coulomb-screened self-energy shift at the two-photon level in the  $1s^2$  state of some heliumlike ions, in units of meV. Here WF refers to the wave-function correction which corresponds to the part with only intermediate  $Q$  states, MSC to the model-space contribution, and VTX to the vertex correction.

|                                    |               |               |
|------------------------------------|---------------|---------------|
| $Z = 14$                           | Coulomb gauge | Feynman gauge |
| WF zero-potential term             | -64.7(7)      | 1498.3(7)     |
| WF one-potential term              | 2.70(2)       | -1149.16(4)   |
| WF many-potential term             | 5.583(4)      | -396.046(5)   |
| Sum                                | -56.4(7)      | -46.9(7)      |
| MSC zero-potential term            | -14.64(1)     | 3467.4(1)     |
| VTX zero-potential term            | 10.42(1)      | -3327.6(1)    |
| MSC + VTX higher-order terms       | -0.57(1)      | -153.9(5)     |
| Sum                                | -4.79(3)      | -14.1(7)      |
| Total Coulomb-screened self-energy | -61.2(7)      | -61(1)        |
| $Z = 18$                           | Coulomb gauge | Feynman gauge |
| WF zero-potential term             | -115.8(7)     | 1620.8(6)     |
| WF one-potential term              | 0.441(4)      | -1218.16(4)   |
| WF many-potential term             | 11.111(5)     | -489.559(6)   |
| Sum                                | -104.2(7)     | -86.9(6)      |
| MSC zero-potential term            | -24.79(2)     | 3819.0(1)     |
| VTX zero-potential term            | 16.21(2)      | -3653.3(1)    |
| MSC + VTX higher-order terms       | -1.07(2)      | -192.2(6)     |
| Sum                                | -9.65(6)      | -26.5(8)      |
| Total Coulomb-screened self-energy | -113.8(8)     | -113(1)       |
| $Z = 24$                           | Coulomb gauge | Feynman gauge |
| WF zero-potential term             | -221.4(6)     | 1722.3(3)     |
| WF one-potential term              | -11.1(1)      | -1279.37(5)   |
| WF many-potential term             | 24.059(7)     | -617.076(9)   |
| Sum                                | -208.4(7)     | -174.1(4)     |
| MSC zero-potential term            | -43.22(4)     | 4164.5(1)     |
| VTX zero-potential term            | 24.12(4)      | -3972.3(1)    |
| MSC + VTX higher-order terms       | -2.16(4)      | -246.9(8)     |
| Sum                                | -21.3(1)      | -54.7(10)     |
| Total Coulomb-screened self-energy | -229.7(8)     | -229(1)       |
| $Z = 30$                           | Coulomb gauge | Feynman gauge |
| WF zero-potential term             | -360.4(4)     | 1758.44(7)    |
| WF one-potential term              | -37.0(4)      | -1322.11(5)   |
| WF many-potential term             | 43.33(1)      | -733.10(1)    |
| Sum                                | -354.1(8)     | -296.8(1)     |
| MSC zero-potential term            | -63.6(1)      | 4362.4(1)     |
| VTX zero-potential term            | 28.3(1)       | -4158.8(1)    |
| MSC + VTX higher-order terms       | -3.71(6)      | -299(1)       |
| Sum                                | -39.0(3)      | -95.3(10)     |
| Total Coulomb-screened self-energy | -393(1)       | -392(1)       |
| $Z = 50$                           | Coulomb gauge | Feynman gauge |
| WF zero-potential term             | -1046.1(1)    | 1650.9(7)     |
| WF one-potential term              | -307(3)       | -1572.45(5)   |
| WF many-potential term             | 162.4(9)      | -1088.9(1)    |
| Sum                                | -1191(4)      | -1010.5(9)    |
| MSC zero-potential term            | -117.1(2)     | 4458.9(1)     |
| VTX zero-potential term            | -24.9(1)      | -4328.7(1)    |
| MSC + VTX higher-order terms       | -15.2(3)      | -473(2)       |
| Sum                                | -157.2(6)     | -342(2)       |
| Total Coulomb-screened self-energy | -1348(5)      | -1352(3)      |

puted in coordinate space from the bound-state QED Feynman rules as the difference between the diagrams with bound propagators and free propagators using a partial-wave expansion of the photon.

Upon extrapolation to continuous space and to an infinite summation limit in partial waves  $l$ , the uncertainty of the individual diagrams on the left-hand side in Fig. 5 is on the 0.1% level for the self-energy correction. This uncertainty

is of the same absolute magnitude as the very effects we wish to compute. A drastic improvement can be obtained by carrying out the subtraction for each set of grid and summation parameters before any extrapolation is performed. The result from this subtraction can then be extrapolated with a relative uncertainty which is on the order of 1% for the self-energy.

#### IV. RESULTS AND DISCUSSION

In this section we give numerical results for the combined effect of arbitrarily many Coulomb interactions together with a one-photon QED perturbation. The self-energy and vacuum-polarization contributions are calculated in this work and the corresponding contribution for the exchange of a single transverse photon was calculated in [14]. For comparison we have computed all the self-energy corrections in this work using both Coulomb gauge and Feynman gauge.

As mentioned above, our computational scheme requires the computation of diagrams at the two-photon level (one Coulomb interaction together with a single retarded photon). In Table II we present results for the contributions to the Coulomb-screened self-energy shift in the  $1s^2$  state of some heliumlike ions, as obtained in the Coulomb gauge and the Feynman gauge. We note that the contributions in Coulomb gauge behave in a physically intuitive way: the higher-order terms act as small corrections to the zeroth-order terms. The Feynman gauge, by comparison, is characterized by a large degree of cancellation in general and large contributions from higher-order terms. In Table III we compare the total shift we obtain to results given in the literature.

In Table IV we give results for the energy shift (24) due to the combined effect of correlation and self-energy (effects beyond the two-photon level). The shift is calculated in the Coulomb and Feynman gauges to allow comparison. The contributions we have calculated behave quite differently in the two gauges and it is interesting to note the unphysical  $Z$  behavior of the Feynman gauge. In absolute terms, we expect the combined effect of correlation and self-energy beyond the two-photon level (including MSC and vertex corrections) to scale roughly as  $1/Z^2$  since it differs from the self-energy screened by a single photon by an extra  $(1/Z)$  Coulomb interaction. This is not at all the case for the Feynman-gauge contributions we have calculated here;

TABLE III. Results for Coulomb-screened self-energy at the two-photon level obtained in this work compared to values in the literature. For comparison the fifth column shows values for the complete screened self-energy, including the transverse part of the exchanged photon. Units are meV.

| Z  | Coulomb gauge | Feynman gauge | Other authors       | Other authors (including Breit-screening)     |
|----|---------------|---------------|---------------------|---|
| 14 | -61.2(7)      | -61(1)        |                     | -59.6(2) <sup>b</sup>                         |
| 18 | -113.8(8)     | -113(1)       | -113.8 <sup>a</sup> | -111.6 <sup>a</sup> , -111.60(2) <sup>b</sup> |
| 24 | -229.7(8)     | -229(1)       | -230.1 <sup>a</sup> | -227.8 <sup>a</sup>                           |
| 30 | -393(1)       | -392(1)       |                     | -396.51(6) <sup>b</sup>                       |
| 50 | -1348(5)      | -1352(3)      |                     | -1471.7(1) <sup>b</sup>                       |

<sup>a</sup>Sunnergren [25].

<sup>b</sup>Artemyev *et al.* [5].

TABLE IV. Self-energy contributions to the combined QED-correlation energy shift beyond the two-photon level in the  $1s^2$  state of some heliumlike ions. The abbreviations are similar to those in Table II. All values are given in units of meV.

| Z                       | Coulomb gauge | Feynman gauge |
|-------------------------|---------------|---------------|
| <b>Z = 14</b>           |               |               |
| Without MSC or vertex   |               |               |
| -zero-potential term    | 3.47(3)       | -164.82(3)    |
| -one-potential term     | -0.0275(2)    | 71.80(3)      |
| -many-potential term    | -0.451(3)     | 12.170(4)     |
| -sum                    | 2.99(4)       | -80.85(6)     |
| MSC zero-potential term | 0.87          | -30.7         |
| VTX zero-potential term | -0.63         | 66.5          |
| Total sum               | 3.23(4)       | -45.05(6)     |
| <b>Z = 18</b>           |               |               |
| Without MSC or vertex   |               |               |
| -zero-potential term    | 4.79(2)       | -142.39(2)    |
| -one-potential term     | 0.143(1)      | 59.7(5)       |
| -many-potential term    | -0.691(4)     | 11.569(3)     |
| -sum                    | 4.24(3)       | -71.1(5)      |
| MSC zero-potential term | 1.16          | -24.3         |
| VTX zero-potential term | -0.73         | 54.2          |
| Total sum               | 4.67(3)       | -41.2(5)      |
| <b>Z = 24</b>           |               |               |
| Without MSC or vertex   |               |               |
| -zero-potential term    | 6.77(2)       | -118.482(5)   |
| -one-potential term     | 0.585(6)      | 47.8(4)       |
| -many-potential term    | -1.104(6)     | 10.79(2)      |
| -sum                    | 6.25(3)       | -59.9(4)      |
| MSC zero-potential term | 1.54          | -17.6         |
| VTX zero-potential term | -0.76         | 41.6          |
| Total sum               | 7.03(3)       | -35.9(4)      |
| <b>Z = 30</b>           |               |               |
| Without MSC or vertex   |               |               |
| -zero-potential term    | 8.702(8)      | -101.507(2)   |
| -one-potential term     | 1.22(1)       | 40.2(1)       |
| -many-potential term    | -1.569(9)     | 10.250(6)     |
| -sum                    | 8.36(3)       | -51.1(1)      |
| MSC zero-potential term | 1.82          | -13.0         |
| VTX zero-potential term | -0.61         | 33.2          |
| Total sum               | 9.57(3)       | -30.9(1)      |
| <b>Z = 50</b>           |               |               |
| Without MSC or vertex   |               |               |
| -zero-potential term    | 14.823(2)     | -69.641(1)    |
| -one-potential term     | 5.17(5)       | 29.88(2)      |
| -many-potential term    | -3.30(2)      | 19.29(1)      |
| -sum                    | 16.69(7)      | -20.47(3)     |
| MSC zero-potential term | 2.15          | -4.9          |
| VTX zero-potential term | 1.10          | 19.4          |
| Total sum               | 19.94(7)      | -5.97(3)      |

instead they actually decrease with increasing  $Z$ . This suggests that a complete treatment including the higher-order MSC and vertex-correction terms is needed to get sensible results in this gauge. The corresponding Coulomb-gauge values, on the other hand, show a  $Z$  dependence which is closer to the expected one.

The energy shifts due to the combined QED-correlation effects beyond the two-photon level are compiled in Table V for all the one-photon QED perturbations considered in this work (single transverse-photon exchange, self-energy, and



TABLE V. Contributions to the combined QED-correlation energy shift beyond the two-photon level in the  $1s^2$  state of some heliumlike ions. In the rightmost column we sum all contributions except the instantaneous Breit part. All values are given in meV.

| Z  | Transverse photon<br>(instantaneous Breit) | Transverse photon<br>(retardation effect) | Self-energy | Vacuum polarization | Total QED-correlation effect |
|----|--|---|-------------|---------------------|------------------------------|
| 14 | 8.19                                       | -1.86                                     | 3.2(1)      | -0.136              | 1.2(1)                       |
| 18 | 10.13                                      | -2.73                                     | 4.7(1)      | -0.225              | 1.7(1)                       |
| 24 | 12.73                                      | -4.16                                     | 7.0(2)      | -0.402              | 2.5(2)                       |
| 30 | 15.03                                      | -5.71                                     | 9.6(3)      | -0.639              | 3.3(3)                       |
| 50 | 21.46                                      | -11.47                                    | 19.9(7)     | -2.093              | 6.3(7)                       |

vacuum polarization). The single transverse-photon exchange contributions are gathered from [14], and the self-energy contributions are approximated as the sum of the calculated Coulomb-gauge terms in Table IV. The total uncertainty of the self-energy contribution is calculated as the sum of the numerical uncertainty and the estimated size of the omitted higher-order MSC and vertex terms. At the two-photon level (Table II) the higher-order terms represent roughly 10% of the total MSC + vertex contribution in Coulomb gauge, and we thus expect an additional uncertainty from the uncalculated terms taken as 20% of the MSC+vertex zero-potential terms to be conservative in the correlated case. In the rightmost column of Table V we have summed the contributions from the self-energy, vacuum polarization, and the retardation effect of the single-photon exchange, which are the effects normally considered as QED effects in the context of MBPT. The magnitude and relative sign of the self-energy correction as compared to the vacuum polarization agrees with what one finds in lower orders, and this further supports our approximative treatment of the self-energy in Coulomb gauge.

In addition to the effects considered in this work there are corrections from intermediate negative-energy states, an effect which lies beyond the no-virtual-pair approximation and traditionally belongs to the class of QED effects. This effect is not very important when considered together with only Coulomb interactions, but contributes significantly together with transverse-photon interactions (see, e.g., [26]). Calculations of the combined effect of Coulomb-correlation and single-photon exchange together with virtual pairs based on the generalized potential (28) were performed in [14], and the magnitude of the combined effect of retardation and correlation beyond the two-photon level (column 3 in Table V) was found to decrease by roughly 20% for all the values

TABLE VI. Total combined QED-correlation effect in the  $1s^2$  state of heliumlike ions compared to the higher-order QED effect from [5]. The second column gives our results in the no-virtual-pair approximation. The third column gives the estimated results after including virtual pairs. In units of meV.

| Z  | QED-correlation<br>NVP | QED-correlation<br>with VP (estimated) | Artemyev $\Delta E_{ho}^{QED}$ |
|----|------------------------|--|--------------------------------|
| 14 | 1.2(1)                 | 1.0(1)                                 | 0.8                            |
| 18 | 1.7(1)                 | 1.4(1)                                 | 0.9                            |
| 24 | 2.5(2)                 | 2.0(2)                                 |                                |
| 30 | 3.3(3)                 | 2.6(3)                                 | -0.2                           |
| 50 | 6.3(7)                 | 5.0(7)                                 | -7.7(50)                       |

of  $Z$  considered. The corresponding correction from virtual pairs to correlation combined with self-energy or vacuum polarization has not yet been studied, but one might expect a correction of the same order, namely, a reduction of the total QED-correlation effect by 20%.

Although not exactly equivalent, our results for the combined correlation and QED shift can be compared with the higher-order QED correction in Artemyev *et al.* [5] which was calculated using the unified method of Drake [4] (see Table VI). The second column in Table VI is taken from Table V and in the third column we have estimated the inclusion of virtual pairs by multiplying our results by a factor of 0.8 based on the discussion above. We see that for  $Z = 14$  and 18 the agreement with [5] is close but our results tend to be a bit larger. For  $Z = 24$  no value is specified in [5] but the result we obtain here is more than twice as large in magnitude as the uncertainty of the total ionization energy given in that work. A severe disagreement is, however, seen for  $Z = 30$  and  $Z = 50$  which might be due to an increasing importance of relativistic effects in the electron correlation for heavier nuclei, effects that are included to a large extent in this work due to the use of a relativistic Dirac model Hamiltonian (12) while the method of [4] is based on a nonrelativistic treatment of electron correlation. For  $Z = 30$  the correction we find is of the same size as the uncertainty of the total ionization energy obtained in [5], and for  $Z = 50$  it is a factor of 2 smaller.

Finally, we wish to make a comment regarding the  $Z$ -dependent discrepancy between theory and experiment which has recently been claimed to have been observed by Chantler *et al.* in a compilation of measured transition energies for the  $1s2p(^1P_1) \rightarrow 1s1s(^1S_0)$  transition in heliumlike ions [27]. Our results seem to rule out an explanation of such a discrepancy in terms of the combination of correlation and QED effects since (1) the magnitude of the correction we obtain is about a factor of 100 smaller than the discrepancy found in [27], and (2) the sign of the correction leads to an increase in energy of the  $1s1s$  level and thus to a *decrease* in the transition energy (the combined corrections considered here can be expected to have a negligible effect on the  $1s2p$  state), while Chantler *et al.* claim to see larger transition energies compared to theory.

## V. CONCLUSION

We have computed the combined effect of electron correlation together with electron self-energy and vacuum polarization in the energy of the ground state of heliumlike heavy ions. Together with previously calculated values for the combination of correlation and single-photon exchange, this

has allowed us to obtain the energy shift due to first-order QED effects combined with electron correlation. We have also presented a detailed analysis of the contributions to the Coulomb-screened self-energy correction at the two-photon level in the Coulomb and Feynman gauges. It was found that an overall feature of the self-energy corrections in Coulomb gauge is that most of the effect is located in the zero-potential terms, with the higher-order terms acting as minor corrections. This is not at all the case in the Feynman gauge where often the higher-order terms dominate over the zero-potential

terms. Moreover, we have seen that an incomplete treatment of the self-energy corrections in Feynman gauge may lead to completely unphysical  $Z$  scalings.

#### ACKNOWLEDGMENTS

The authors thank Daniel Hedendahl for permission to publish results from his Ph.D. thesis. J.H. acknowledges support from the Helmholtz Association and GSI under Project VH-NG-421.

- 
- [1] P. Indelicato, O. Gorcex, and J. Desclaux, *J. Phys. B* **20**, 651 (1987).
  - [2] K. T. Cheng, M. H. Chen, W. R. Johnson, and J. Sapirstein, *Phys. Rev. A* **50**, 247 (1994).
  - [3] K. T. Cheng and M. H. Chen, *Phys. Rev. A* **61**, 044503 (2000).
  - [4] G. W. Drake, *Can. J. Phys.* **66**, 586 (1988).
  - [5] A. N. Artemyev, V. M. Shabaev, V. A. Yerokhin, G. Plunien, and G. Soff, *Phys. Rev. A* **71**, 062104 (2005).
  - [6] V. M. Shabaev, *Phys. Rep.* **356**, 119 (2002).
  - [7] J. Sucher, *Phys. Rev.* **107**, 1448 (1957).
  - [8] I. Lindgren, S. Salomonson, and B. Åsén, *Phys. Rep.* **389**, 161 (2004).
  - [9] I. Lindgren, *Relativistic Many-Body Theory: A New Field-Theoretical Approach* (Springer-Verlag, New York, 2011).
  - [10] I. Lindgren, S. Salomonson, and D. Hedendahl, *Phys. Rev. A* **73**, 062502 (2006).
  - [11] I. Lindgren, S. Salomonson, and D. Hedendahl, *Can. J. Phys.* **83**, 183 (2005).
  - [12] I. Lindgren, S. Salomonson, and D. Hedendahl, *J. At. Mol. Opt. Phys.* **2011**, 723574 (2011).
  - [13] I. Lindgren and J. Morrison, *Atomic Many-Body Theory* (Springer-Verlag, Berlin, 1986).
  - [14] D. Hedendahl, Ph.D. thesis, University of Gothenburg, 2010.
  - [15] S. Salomonson and P. Öster, *Phys. Rev. A* **40**, 5559 (1989).
  - [16] S. Salomonson and P. Öster, *Phys. Rev. A* **40**, 5548 (1989).
  - [17] I. Lindgren, B. Åsén, S. Salomonson, and A. Mårtensson-Pendrill, *Phys. Rev. A* **64**, 062505 (2001).
  - [18] N. J. Snyderman, *Ann. Phys. (N.Y.)* **211**, 43 (1991).
  - [19] S. A. Blundell and N. J. Snyderman, *Phys. Rev. A* **44**, R1427 (1991).
  - [20] D. Hedendahl and J. Holmberg, *Phys. Rev. A* **85**, 012514 (2012).
  - [21] J. Holmberg, *Phys. Rev. A* **84**, 062504 (2011).
  - [22] W. Greiner, B. Müller, and J. Rafelski, *Quantum Electrodynamics of Strong Fields* (Springer-Verlag, Berlin, 1985).
  - [23] A. G. Fainshtein, N. L. Manakov, and A. A. Nekipelov, *J. Phys. B: At. Mol. Opt. Phys.* **24**, 559 (1991).
  - [24] P. Sunnergren, H. Persson, S. Salomonson, S. M. Schneider, I. Lindgren, and G. Soff, *Phys. Rev. A* **58**, 1055 (1998).
  - [25] P. Sunnergren, Ph.D. thesis, University of Gothenburg, 1998.
  - [26] I. Lindgren, H. Persson, S. Salomonson, and L. Labzowsky, *Phys. Rev. A* **51**, 1167 (1995).
  - [27] C. T. Chantler, M. N. Kinnane, J. D. Gillaspay, L. T. Hudson, A. T. Payne, L. F. Smale, A. Henins, J. M. Pomeroy, J. N. Tan, J. A. Kimpton *et al.*, *Phys. Rev. Lett.* **109**, 153001 (2012).